AD-A125 548 MECHANICAL PROPERTIES OF THE SPINAL LIGAMENTS OF PRIMATES 1 CYCLIC LOADIN..(U) MICHIGAN STATE UNIV EAST LANSING DEPT OF BIOMECHANICS R W LITTLE ET AL. FEB 83 1/1

UNCLASSIFIED AFAMRL-TR-83-0005 F33615-79-C-0514 F/G 6/19 NL

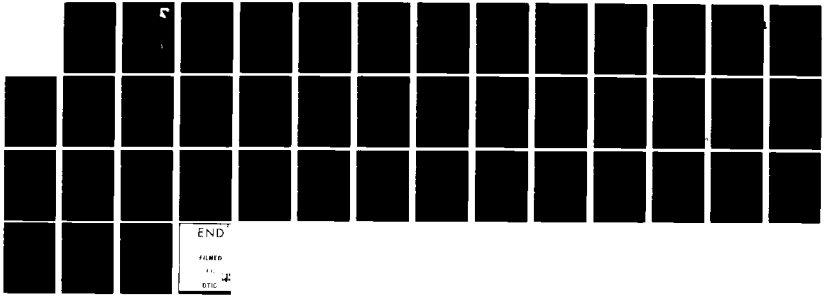

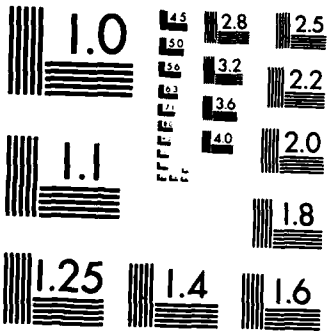

AFAMRL-TR-83-0005

12

MECHANICAL PROPERTIES OF THE SPINAL LIGAMENTS OF PRIMATES: FINAL REPORT

1. CYCLIC LOADING

2. MATHEMATICAL MODELING

ROBERT WM. LITTLE, PhD
ROBERT P. HUBBARD, PhD
MICHIGAN STATE UNIVERSITY
EAST LANSING, MICHIGAN 48824

ARNOLD R. SLONIM, PhD
AIR FORCE AEROSPACE MEDICAL RESEARCH LABORATORY

FEBRUARY 1983

AIR FORCE AEROSPACE MEDICAL RESEARCH LABORATORY
AEROSPACE MEDICAL DIVISION
AIR FORCE SYSTEMS COMMAND
WRIGHT-PATTERSON AIR FORCE BASE, OHIO 45433

NOTICES

When US Government drawings, specifications, or other data are used for any purpose other than a definitely related Government procurement operation, the Government thereby incurs no responsibility nor any obligation whatsoever, and the fact that the Government may have formulated, furnished, or in any way supplied the said drawings, specifications, or other data, is not to be regarded by implication or otherwise, as in any manner licensing the holder or any other person or corporation, or conveying any rights or permission to manufacture, use, or sell any patented invention that may in any way be related thereto.

Please do not request copies of this report from Air Force Aerospace Medical Research Laboratory. Additional copies may be purchased from:

National Technical Information Service
5285 Port Royal Road
Springfield, Virginia 22161

Federal Government agencies and their contractors registered with Defense Technical Information Center should direct requests for copies of this report to:

Defense Technical Information Center
Cameron Station
Alexandria, Virginia 22314

TECHNICAL REVIEW AND APPROVAL

AFAMRL-TR-83-005

This report has been reviewed by the Office of Public Affairs (PA) and is releasable to the National Technical Information Service (NTIS). At NTIS, it will be available to the general public, including foreign nations.

This technical report has been reviewed and is approved for publication.

FOR THE COMMANDER

HENNING E. VON GIERKE, Dr Ing
Director
Biodynamics and Bioengineering Division
Air Force Aerospace Medical Research Laboratory

SECURITY CLASSIFICATION OF THIS PAGE *(When Data Entered)*

REPORT DOCUMENTATION PAGE

READ INSTRUCTIONS BEFORE COMPLETING FORM

1. REPORT NUMBER AFAMRL-TR-~~82~~ 83-0005	2. GOVT ACCESSION NO. A125540
3. RECIPIENT'S CATALOG NUMBER	
4. TITLE *(and Subtitle)* MECHANICAL PROPERTIES OF THE SPINAL LIGAMENTS OF PRIMATES: FINAL REPORT 1. CYCLIC LOADING 2. MATHEMATICAL MODELING	5. TYPE OF REPORT & PERIOD COVERED Technical Report
	6. PERFORMING ORG. REPORT NUMBER
7. AUTHOR(s) Robert Wm. Little, Ph.D. Robert P. Hubbard, Ph.D. Arnold R. Slonim, Ph.D.	8. CONTRACT OR GRANT NUMBER(s) F33615-79-C-0514
9. PERFORMING ORGANIZATION NAME AND ADDRESS Biomechanics Department Michigan State University East Lansing, Michigan 48824-1316	10. PROGRAM ELEMENT, PROJECT, TASK AREA & WORK UNIT NUMBERS 62202F, 7231-14-09
11. CONTROLLING OFFICE NAME AND ADDRESS Air Force Aerospace Medical Research Laboratory, Aerospace Medical Division, Air Force Systems Command, Wright-Patterson AFB, OH 45433	12. REPORT DATE 13. NUMBER OF PAGES
14. MONITORING AGENCY NAME & ADDRESS(*if different from Controlling Office*)	15. SECURITY CLASS. *(of this report)* Unclassified 15a. DECLASSIFICATION/DOWNGRADING SCHEDULE NA

16. DISTRIBUTION STATEMENT *(of this Report)*

Approved for public release; distribution unlimited.

17. DISTRIBUTION STATEMENT *(of the abstract entered in Block 20, if different from Report)*

18. SUPPLEMENTARY NOTES

AFAMRL Contract Monitor: Dr. A. R. Slonim, AFAMRL/BBD, Tel 513-255-3242

19. KEY WORDS *(Continue on reverse side if necessary and identify by block number)*

Spinal Ligaments	Failure	Baboon
Mechanical Stress	Creep	Human
Biomechanical Response	Mathematical Modeling	Spinal Injuries
Material Property Characteristics	Constitutive Equation	Vibratory Load
Cyclic Loading	Rhesus Monkey	Animal Models

20. ABSTRACT *(Continue on reverse side if necessary and identify by block number)*

The two parts of this report cover an experimental investigation of the extension and failure of spinal ligaments to cyclic loading and a mathematical model of spinal ligament responses to specified strain histories. This concludes a three-year effort to measure and model the viscoelastic properties of spinal ligaments from rhesus monkeys, baboons, chimpanzees, and humans. Information on the mechanical properties of spinal ligaments is essential to an understanding of the mechanism by which air crew personnel experience spinal injuries in vibratory loading environments and emergency situations. (continued)

DD FORM 1 JAN 73 1473 EDITION OF 1 NOV 65 IS OBSOLETE

SECURITY CLASSIFICATION OF THIS PAGE *(When Data Entered)*

Block 20. Abstract (cont'd)

In Part 1, the extension and failure responses of anterior longitudinal, posterior longitudinal, ligamentum flavum, and supraspinous ligament samples were measured for single extensions and cyclic loading. Effects of cyclic loading on failure stress and cyclic creep extension responses were evaluated.

In Part 2, a mathematical constitutive equation was developed with a linear viscoelastic model for individual ligament fibers integrated with a distribution function to include effects of variation in fiber orientation, extension for initial loading, and extension response. Coefficients controlling tissue response were determined by numerical solution of the constitutive equation using the fastest strain rate data. Then analytical and experimental results were compared for selected human spinal ligament samples.

SUMMARY

This report is composed of two parts covering the response of spinal ligaments to cyclic creep and a mathematical model of those ligaments to a specified strain history. This concludes a three-year endeavor to determine the properties of spinal ligaments from rhesus monkey, baboon, chimpanzee and human specimens.

Four ligaments of the spine of rhesus monkey and baboon were selected for testing in Part 1 with test samples taken at different vertebral levels. The cyclic creep tests on ligaments from three rhesus monkeys and two baboons were preceded by single extension failure tests on ligaments from two rhesus monkeys to establish a range of static failure.

As described in Part 2, a mathematical constitutive equation was developed using a linear viscoelastic model for individual fibers and a distribution function to include the effects of fiber distribution, orientation and initial length. Material constants and the distribution function were determined by numerical solution of the constitutive integral equation using the fastest strain rate data. Analytical and experimental results were compared for selected human spinal ligament samples.

This research completes an initial investigation of the mechanical properties of spinal ligaments and ligaments from the lower extremities. Research of this nature is necessary to understand the mechanism of injuries in aircrewmen that result from exposure to vibratory loading environments and high stress or strain rates during escape and crash episodes. Determining the tissue response differences between different primate species will aid in the selection of animal models and in development of the interspecies scaling techniques to establish criteria and of preventive measures for the safety of aircrews.

PREFACE

The research documented in this report was performed in the Department of Biomechanics, College of Osteopathic Medicine, Michigan State University, East Lansing, Michigan 48824, under AF Contract No. F33615-79-C-0514. Dr. Robert William Little, Professor and Chairman of the Department, was the Principal Investigator; Dr. Robert P. Hubbard was the Co-investigator. The research reported herein, representing the last phase of this three-year effort, was conducted in support of Work Unit 72311409, "Mechanical Stress on Soft Tissue Material Properties." Dr. Arnold R. Slonim, Biodynamic Effects Branch, Biodynamics and Bioengineering Division, Air Force Aerospace Medical Research Laboratory, was the project scientist and contract monitor.

The authors gratefully acknowledge the contributions of Michael Sacks, Mary Verstraete, Dorothee Rometsch, Janet Frahm, Glenn Beavis, and Richard Geist to the conduct of the ligament testing and data analysis in Part 1 and the work of Mary Verstraete in the theoretical analysis in Part 2. The assistance of Laura Hayes and Ann Eschtruth in the preparation of this report is greatly appreciated.

The cooperation and assistance of Colonel A. R. Banknieder and Major John G. Golden of the Veterinary Sciences Division, Air Force Aerospace Medical Research Laboratory, and of Dr. Charles E. Graham, Deputy Director, Primate Research Institute, New Mexico State University at Holloman AFB, New Mexico, in providing primate cadaveric specimens vital to this study are very much appreciated.

TABLE OF CONTENTS

LIST OF ILLUSTRATIONS

LIST OF TABLES

INTRODUCTION

Biological tissues are viscoelastic so that their responses to a current loading or deformation are affected by their mechanical environment before the current time. Loading and deformation of tissues occur continuously by exercise or inputs from outside the body. The continuous nature of demands on tissues and the dependence of tissue response on previous demands lead to significant questions concerning the effects of repeated loading on tissue deformation and failure. For example, what are the effects of vigorous exertion or severe mechanical inputs on the potential for injury of a pilot in an emergency situation? In studying and modelling the biodynamic response of the pilot, how are the responses of tissues, and the modelling elements which represent them, affected by repeated loading?

The load relaxation response to a few extension cycles has been used to evaluate the validity of constitutive models for soft connective tissues; typical among such studies are the works of Haut and Little[1] and Woo, Gomez, and Akeson[2] which are based on the viscoelastic theories of Fung.[3] Lanir[4] has proposed a model for soft connective tissues that incorporates the approach of Fung[3] with a distribution of tissue fiber lengths. A similar model is presented and discussed in Part 2 of this report. Lanir[4] predicts load relaxation responses to constant and cyclic extensions and the creep extension responses to constant and cyclic loading; however, no experimental evaluations of tissue behaviors have been made of Lanir's model, nor has the model presented in this report been compared with experimental data for cyclic creep.

The creep extension of human digital tendon was studied by Cohen et al.,[5] with particular attention to the activation energy for the viscoelastic mechanism. They found creep strain rate to be roughly proportional to stress raised to a positive power less than one. The creep extension of passive cardiac muscle was measured by Pinto and Fung[6] and was found to be roughly a linear function of logarithm of time. The bending deformation and recovery due to application and removal of loading on fresh human lumbar spines were recorded by Twomey and Taylor.[7]

The previous research on creep of connective tissues was very limited in extent and included no data on creep deformation due to cyclic loading or on the effects of repeated loading on tissue failure.

The current study reported in Part 1 was undertaken to obtain initial data for the effects of repeated loading on the deformation and failure of spinal ligaments. The approach to this research was modelled after the study of metal fatigue in which material samples are failed by single extensions or by repeated loading, and the failure loads are normalized by sample area to obtain plots of stress versus number of cycles to failure.

The goals of Part 1 of the research were to:

a. Study the effects of cyclic loading on the failure of spinal ligaments;
b. Study the sample extensions due to the cyclic loading, i.e., cyclic creep.

The goal of Part 2 was to model selected spinal ligaments in terms of their anatomical microstructure (including fibral composition and orientation) as well as their biomechanical response.

PART 1

CYCLIC LOADING OF SPINAL LIGAMENTS FROM RHESUS MONKEYS AND BABOONS

METHODS AND MATERIALS

Spinal ligament samples from two rhesus monkeys were pulled to failure in single extensions, and spinal ligament samples from three additional rhesus monkeys and two baboons were subjected to cyclic loading and failure. The methods used in preparing the spinal ligaments for testing and in sample gripping were the same as in previous mechanical testing of spinal ligaments.[8] That is, the spinal column was removed from an eviscerated primate, sectioned into vertebral pairs for testing and histology according to Figure 1, and sectioned further into bone-ligament-bone samples containing either the anterior longitudinal ligament (A.L.L.), posterior longitudinal ligament (P.L.L.), ligamentum flavum (L.F.), or supraspinous ligament (S.S.L.). As in previous studies,[8] the samples were gripped by clamping the vertebral bone segments between fixtures with waterproof sanding mesh of 80 grit; the ligament cross-sectional areas were measured using histological sections.

The spinal ligament samples from two rhesus monkeys were extended to failure. These failure loads were normalized by ligament cross-sectional area resulting in failure stress and were used to estimate the failure loads for the other ligament samples that were loaded repeatedly.

Ligament lengths were approximated as the bone-to-bone distances when samples were mounted in the testing grips and extended to onset of loading. Based on these estimates of ligament length, the deflection rates for the single-extension failure tests were selected to produce 1%/s strain rate and resulted in an average stress rate of 2 MPa/s based on failure stress and test duration. Since the samples stiffen, the stress rate at failure would be higher than this average.

A testing protocol was developed to subject the ligament samples to repeated cycles of load with sample loading controlled to vary between minimum and maximum values that were less than the estimated single-extension failure load. The stress levels in this cyclic testing could only be estimated; exact stress values were determined after histological studies of ligament areas were conducted. The cyclic tests were run with the load sinusoidally ranging from the maximum load to an average of 0.65 of that maximum; that is an average of about 20% cyclic variation in load from a constant mean load. The average cyclic stress rate was 22 MPa/s, which was superimposed on the mean stress level. The cyclic stress rate was about ten times greater than the stress rate in the failure tests by single extension. The fact that the cyclic stress was superimposed on a constant stress makes the comparison of stress rates between test types difficult. However, increased loading rate is known to increase failure loads in ligaments[9] and increase the likelihood of bone failure in bone-ligament-bone samples.

Samples from the first animal tested were loaded cyclically to failure or it was apparent that they would not fail at that loading level, and the test was stopped. Later, samples were cycled at chosen load levels until they failed or for about 4,000 cycles after which they were extended to failure.

The testing was performed with a servohydraulic materials testing system, and the entire cyclic testing protocol was controlled and recorded by digital computer. Once the sample was mounted in the testing grips and appropriate testing parameters, such as sample identification and loading limits, had been entered into the computer, the sample was extended under stroke control to the minimum load for cyclic testing; and then the testing machine was transferred to load control for cyclic loading. All these tests were run at a frequency of one cycle per second. The tests were started in stroke control to avoid possible servocontrol instability in load control with a sample of low initial stiffness.

During the cyclic testing, load and extension were recorded with the computer at 50 data pairs per second for about 5 seconds in repeated fifteen second intervals. The sampled data pairs were filtered by a running average of three points and scanned for maximum and minimum values of load and extension. These values, with corresponding times, were then written to the computer disc for storage and subsequent analysis. Thus, the data stored in the computer from each test were maximum and minimum values of load and extension, sampled periodically rather than continuous records of these parameters, which would have been far too extensive for reasonable data storage. In addition to the data stored throughout the test by the computer, the initial 30 seconds of cyclic load and extension were recorded at 50 data pairs per second, using a digital oscilloscope with magnetic storage discs.

The particulars concerning the animals and respective tests are presented in Table 1.

Table 1. Animal Identification Number, Species, Sex, Weight, and Test Type

Identification	Species	Sex	Weight, kg	Test Type
U70	rhesus	male	9.0	failure
U88	rhesus	male	13.9	failure
N75	rhesus	female	7.0	cyclic
A182	rhesus	male	10.0	cyclic
A322	rhesus	male	8.5	cyclic
H-40	baboon	male	14.1	cyclic
H-54	baboon	male	32.7	cyclic

RESULTS

The results from failure testing of spinal ligaments from two rhesus monkeys are given in Tables 2 and 3. By knowing the ligament areas from histological sections adjacent to the tested ligaments, their areas were interpolated and the failure loads were divided by the interpolated cross-sectional areas to calculate failure stress. The failure loads and ligament areas for the larger rhesus (U88) were generally greater than for the smaller animal (U70), so that the failure stresses were similar for same ligament and level in each animal. Large variability in the failure stresses for supraspinous and posterior longitudinal ligaments (S.S.L. and P.L.L., respectively) was due to the small size and indistinct nature of these ligaments in comparison to ligamentum flavum (L.F.) and anterior longitudinal ligaments (A.L.L.). The extensions at failure for the P.L.L. were generally lower than the other ligaments. The L.F. and A.L.L. supported several times more load at failure than P.L.L. or S.S.L. The failure stress and extension data from single extensions to failure will be summarized and compared to such data from cyclic loading later in this part of the report.

After the failure tests by single extension, spinal ligament samples from three rhesus monkeys were subjected to cyclic loading. Stress levels were chosen which were below the stresses that had caused failure of corresponding ligaments in rhesus monkeys U70 and U88. For samples from the first such animal (rhesus N75), the intention was to continue the test until each sample failed during load cycles at less than the single-extension failure stress. As can be seen from Table 4, some of these samples failed immediately or nearly so; some failed after a few hundred cycles; and some endured several thousand cycles. During the testing of the samples from the next animal (rhesus A182), it was decided to limit the number of cycles to 4,000; and if the samples had not failed by then, they would be pulled to failure by a single extension. Thus, for some of the ligaments in the last two rhesus monkeys (A182 and A322), the failure stresses were greater than the maximum cyclic stresses (Tables 5 and 6).

Cyclic loading was also performed with spinal ligaments from two baboons. The maximum cyclic load levels were selected based on failure loads from the rhesus monkeys and were scaled to the baboons by considering the ligament areas. The cyclic tests with the baboon ligaments were run similarly to those of the last two rhesus monkeys; that is, the samples were run for up to 4,000 cycles, and if they had not failed, they were pulled in a single extension to failure. The results of these baboon tests are given in Tables 7 and 8. In Tables 4 through 8, a value of failure stress is given unless the sample did not fail during cyclic loading and was not subsequently extended to failure.

The data from Tables 2 through 8 are presented in Figures 2 through 5 as "stress versus number-of-cycles" plots, commonly used in studies of metal fatigue. The data are grouped by ligament type, i.e. S.L.L., L.F., P.L.L., and A.L.L., and by location, i.e. thoracic (T3-T4, T6-T7, and T9-T10) or lumbar (T12-L1, L2-L3, and L5-L6). The values of failure stresses for single extensions, either by design for the first two animals tested or by chance due to scatter in strength of the ligaments from the

subsequent tests, are plotted with maximum and minimum cyclic stresses and failure stresses at the corresponding number of cycles. The scatter in strength was apparent from these Figures. The ligaments appeared to be as strong after hundreds or thousands of load cycles as t ›v were for a single extension. That is, there did not appear to be any significant effect of cyclic loading on the strength of the spinal ligaments tested. However, the failure loads in the cyclic tests, in comparison to the single extension tests, may have been elevated by the average cyclic stress rate of 22 MPa/s versus 2 MPa/s for the single extension tests.

The failure stresses are summarized in Table 9, and the deflections at which the samples failed are summarized in Table 10, respectively, for the single extensions to failure, cyclic loading, and these two test types combined. The samples have been divided by region into thoracic and lumbar. The variability is either the standard deviation for numbers of samples that are four or greater or range for three samples or less.

In Table 9 there were no significant differences between failure stress levels for the same ligament type due either to location (thoracic versus lumbar) or test type (single extensive versus cyclic loading) with the following exceptions. Lumbar A.L.L. appeared to have a higher failure stress in single extension and cyclic loading than thoracic A.L.L. There were differences in strength between ligament types with the L.F., which is largely elastin, able to resist about half the stress of the other ligaments, which are primarily collagen.

The extensions at failure also indicated no significant effect of cyclic loading compared to single extension or effect of location (thoracic versus lumbar); i.e., any such effects were masked by variability due to other factors. The mean values of failure extension for P.L.L. were consistently less than for the other ligaments.

The cyclic testing of spinal ligaments between maximum and minimum load values resulted in cyclic extensions which increased from cycle to cycle. This extension is cyclic creep. The cyclic extensions were recorded in short-term with the digital oscilloscope for about the first 30 cycles and in long-term with the digital computer every 15 seconds from test initiation until test completion. After trying several mathematical functions, these short- and long-term data were found to be best described by a power function of time:

$$S_n = t^{\beta} \qquad (1)$$

where: S_n is the maximum or minimum extension normalized to the respective value from the first cycle;

t is time measured in seconds;

ß is an exponent.

This function is a straight line through the origin of a plot of logarithm of normalized extension versus logarithm of time with the exponent (ß) as the slope. By taking the logarithm of both sides of equation 1, the following equation is obtained which is used for linear regression with both short- and long-term data sets, i.e., from the digital oscilloscope and from the computer, respectively:

$$\ln S_n = ß[\ln(t)] \qquad (2)$$

The maximum and minimum extensions were normalized by their respective values in the first load cycle and fit to equation 2 with ß equal to B1 for the maximum extensions and ß equal to B2 for the minimum extensions.

The results of the exponential fits are given in Table 11. The correlation coefficients for these regressions were consistently high, typically above 0.97, so there is high confidence that the cyclic creep data are well fit. The exponents B1 and B2 were generally greater for the short-term creep response than the long-term, indicating an initial creep that was more rapid than the responses over hundreds or thousands of load cycles. Although there was variability in the exponents, it was apparent that the creep in the L.F. was less than the other ligaments. This is consistent with the fact that the L.F. is largely elastin, whereas the other ligaments are largely collagen.

The exponent for the extension associated with minimum cyclic load, B2, was generally greater than the exponent for the peak extension, B1. This indicated that the samples were stiffening, with the difference between minimum and peak extension decreasing with repeated cycles of load. The ratio B2/B1 was proportional to the rate of stiffening within the range of numbers of cycles in this study.

PART 2

MATHEMATICAL MODELING

The spinal ligaments have been modeled to reflect both their anatomical microstructure and fibral composition. These ligaments are composed of fibers which vary in initial length and in orientation with the spinal column axis. These variations contribute to the observed non-linear response of the ligaments as the different fibers straighten and become aligned with the loading axis at different strains in the loading history. This observed non-linearity was introduced into the mathematical model by use of a complex distribution function similar to that suggested by Lanir.[4] This distribution function includes the effects of fiber orientation, initial waviness, and distribution.

Each fiber when straightened was considered to be a linearly viscoelastic element satisfying a constitutive equation of the form:

$$\sigma_i(t) = E \int_0^t [1 + \mu \ln(t - \tau + 1)] \frac{\partial \varepsilon_i}{\partial \tau} d\tau \qquad (3)$$

where σ_i is the fiber stress, i is the fiber index, E and μ are fiber material constants, ε_i is the fiber strain, t is a particular time, and τ is the variable time for integration.

Consider a single fiber at an angle θ_i to the loading axis as shown in Figure 6. The fiber is considered to be wavy with an initial length of ℓ_i.

This initial length may be written

$$\ell_i = \frac{x\ (1 + \bar{\varepsilon}_i)}{\cos \theta_i} \qquad (4)$$

where $\bar{\varepsilon}_i$ is the ligament strain at which this ith fiber assumes load corresponding to a ligament deformation of Δx_i. The fiber deformation becomes

$$\Delta_i = (\Delta x - \Delta x_i) \cos \theta_i \qquad (5)$$

and the fiber strain is

$$\varepsilon_i = \frac{(\varepsilon - \bar{\varepsilon}_i)\cos^2\theta_i}{(1 + \bar{\varepsilon}_i)} \tag{6}$$

where ε represents the observed ligament strain.

Substituting equation 6 into equation 3 yields

$$\sigma_i = E\int_{t(\bar{\varepsilon}_i)}^{t} [1 + \mu \ln(t - \tau + 1)] \frac{\partial \varepsilon}{\partial \tau} \frac{\cos^2\theta_i}{(1 + \bar{\varepsilon}_i)} \, d\tau \tag{7}$$

The lower limit of integration corresponds with the time the ith fiber assumes load.

The axial force in the ligament is equal to the sum of the fiber load components.

$$F = \sum_i \sigma_i A_i \cos\theta_i \tag{8}$$

where A_i is the area of the ith fiber.

A complex distribution function $\alpha(\varepsilon)$ will be introduced to include the effects of angle and initial length. The limits of integration for each fiber may be compensated for by use of the Heavyside step function $H(\varepsilon - \eta)$. Substituting equation 7 into equation 8 and integrating over the area yields

$$F = EA\int_0^{\varepsilon} \alpha(\eta) \int_0^{t} [1 + \mu \ln(t - \tau + 1)] H(\varepsilon - \eta) \frac{\partial \varepsilon}{\partial \tau} \, d\tau \, d\eta \tag{9}$$

where A is the total area of the ligament, and ε is the observed ligament strain. The distribution function $\alpha(\varepsilon)$ includes the orientation angle θ_i, preload fiber strain $\bar{\varepsilon}_i$ and fiber area or number A_i. The contribution of each of these factors to the constitutive relation cannot be independently determined. The distribution function is obtained for each ligament by solving the following constitutive equation using the highest constant strain rate data.

$$\sigma = E\int_0^{\varepsilon(t)} \alpha(\eta) \int_0^{t} [1 + \mu \ln(t - \tau + 1)] H(\varepsilon - \eta) \frac{\partial \varepsilon}{\partial \tau} \, d\tau \, d\eta \tag{10}$$

The distribution function can be expanded in a power series in the form

$$\alpha(\eta) = \sum_m C_m \eta^m \tag{11}$$

Substituting this expansion into equation 10 yields

$$\sigma = E \sum_m C_m \int_0^{\varepsilon(t)} \eta^m \int_0^t [1 + \mu \ln(t - \tau + 1)] H(\varepsilon - \eta) \frac{\partial \varepsilon}{\partial \tau} d\tau d\eta \tag{12}$$

This form of the constitutive equation may be integrated for simple strain histories.

Constant strain rate loading:

A constant strain rate loading has a strain history of the form

$$\varepsilon(t) = \beta t \qquad 0 < t < t_1 \tag{13}$$

Substituting into equation 12 yields

$$\sigma(t) = E \sum_m C_m \int_0^t \eta^m \int_0^t [1 + \mu \ln(t - \tau + 1)] H(\tau - \tfrac{\eta}{\beta}) \beta \, d\tau d\eta \tag{14}$$

Integrating gives

$$\sigma(t) = E \sum_m \left\{ C_m \frac{(1 - \mu)(\beta t)^{m+2}}{(m + 1)(m + 2)} + \frac{\mu (\beta t)^{m+2}}{(m + 2)^2} + \mu \beta^{m+2} \frac{(t + 1)^{m+2} \ln(t + 1)}{(m + 1)(m + 2)} \right.$$
$$\left. - \frac{\mu}{(m + 1)(m + 2)} \sum_{k=1}^{m+1} \frac{\beta^k (t + 1)^k (\beta t)^{m-k+2}}{(m - k + 2)} \right\} \tag{15}$$

Hysteresis

The hysteresis strain history involves a constant strain rate loading followed by an unloading at the same rate.

$$\begin{aligned} \varepsilon(t) &= \beta t & 0 < t < t_1 \\ &= \beta(2t_1 - t) & t_1 < t < 2t_1 \end{aligned} \tag{16}$$

Substituting into the constitutive relation yields for the unloading history

$$\sigma(t) = E \sum_m C_m \left\{ \int_0^{\beta(2t_1 - t)} \eta^m \left[\int_{\eta/\beta}^{t_1} [1 + \mu(1 + t - \tau)\, d\tau - \int_{t_1}^{t} [1 + \mu(1 + t - \tau)]\, d\tau \right] d\eta \right\} \tag{17}$$

Integrating yields

$$\sigma(t) = E \sum_m C_m \left\{ \frac{(1 - \mu)(2\beta t_1 - \beta t)^{m+2}}{(m + 1)(m + 2)} + \mu[\beta(2t_1 - t)]^{m+1} \frac{\beta(1 + t)}{(m + 1)} \right.$$

$$- \frac{\beta(2t_1 - t)}{(m + 2)} \ln(1 + 2t - 2t_1) + \frac{\mu[\beta(1 + t)]^{m+2}[\ln(1 + t) - \ln(1 + 2t - 2t_1)]}{(m + 1)(m + 2)}$$

$$- \frac{\mu}{(m + 1)(m + 2)} \sum_{k=1}^{m+1} \left[\beta^k (1 + t)^k \frac{(2\beta t_1 - \beta t)^{m-k+2}}{(m - k + 2)} \right] + \frac{\mu}{(m + 2)^2} (2\beta t_1 - \beta t)^{m-2}$$

$$\left. - \frac{2\mu}{(m + 1)} [\beta(2t_1 - t)]^{m+1} \beta(1 + t - t_1) \ln(1 + t - t_1) \right\} \tag{18}$$

Relaxation

The relaxation strain history may be written

$$\begin{aligned} \varepsilon(t) &= \beta t && 0 < t < t_1 \\ &= \beta t_1 && t > t_1 \end{aligned} \tag{19}$$

The constant strain rate equation is valid for times less than t_1, during the strain ramp. For the relaxation period, $t > t_1$,

$$\sigma(t) = E \sum_m C_m \left\{ \frac{(\beta t_1)^{m+2}\,(1-\mu)}{(m+1)(m+2)} - \frac{\mu}{(m+1)(m+2)} [\beta(1+t)]^{m+2} \ln(1+t-t_1) \right.$$

$$+ \frac{\mu}{(m+1)(m+2)} \left[(\beta t_1)^{m+2} \ln(1+t-t_1) + (\beta\{1+t\})^{m+2} \ln(1+t) \right]$$

$$- \frac{\mu}{(m+1)(m+2)} \sum_{k=1}^{m+2} \frac{(\beta t_1)^{m-k+2} [\beta(1+t)]^k}{(m-k+2)}$$

$$\left. - \frac{\mu}{(m+2)^2} (\beta t_1)^{m+2} \right\} \qquad t > t_1 \qquad (20)$$

The mathematical model was used to predict the response to various strain histories and compared with experimental data. The distribution functions for the human spinal anterior and posterior longitudinal ligaments and the supraspinous ligament are shown in Figure 7. These functions were determined from high strain rate tests by numerical solution of equation 10. These distribution functions were used to predict responses of the different ligaments to particular strain histories. Comparisons of theoretical and experimental data for one human ligament for different strain rate histories are shown in Figures 7 to 10.

LEVEL	TEST
C7 T1	Mechanical
T2	Histological
T3 T4	Mechanical
T5	Histological
T6 T7	Mechanical
T8	Histological
T9 T10	Mechanical
T11	Histological
T12 L1	Mechanical
Interspace	Histological
L2 L3	Mechanical
L4	Histological
L5 L6	Mechanical
L7	Histological

Figure 1: Vertebral Sectioning Scheme for Rhesus and Baboon.

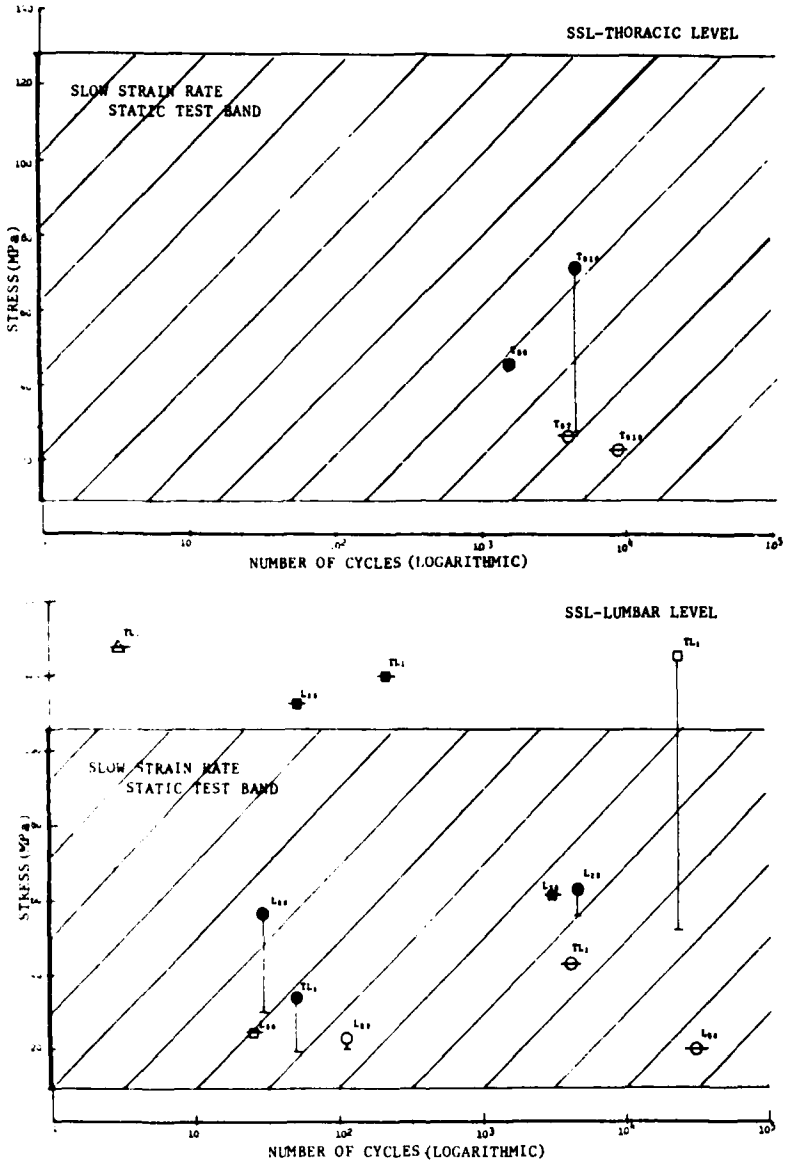

Figure 2: Failure Stress Versus Number of Cycles for Thoracic and Lumbar Supraspinous Ligaments (S.S.L.) from Three Rhesus Monkeys and Two Baboons. The S.S.L. at the thoracic levels (T3-T4, T6-T7, T9-T10) and lumbar levels (T12-L1, L2-L3, L5-L6) were tested in rhesus monkeys A182 (□), N75 (△), and A322 (○) and in baboons H40 (■) and H54 (●). The bar (—) indicates the maximum cyclic stress.

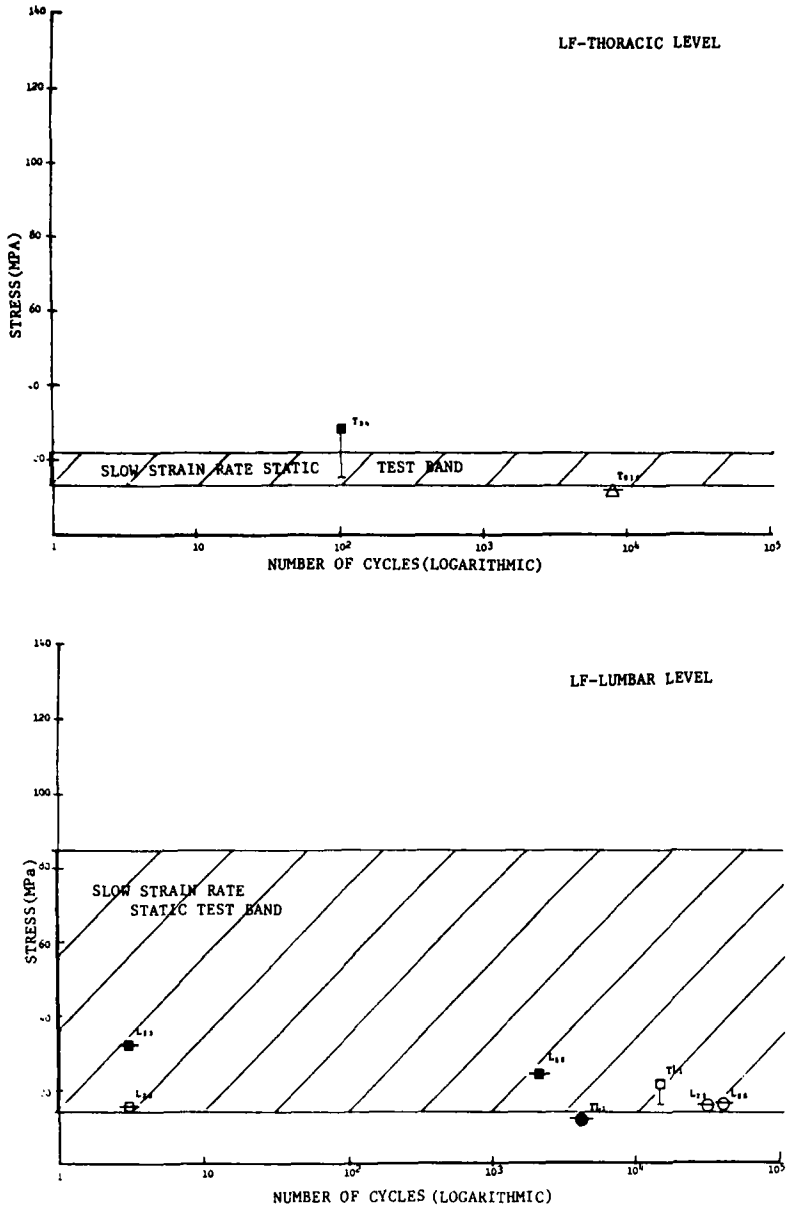

Figure 3: Failure Stress Versus Number of Cycles for Thoracic and Lumbar Ligamenta Flava (L.F.) from Three Rhesus Monkeys and Two Baboons. The L.F. at the thoracic levels (T3-T4, T6-T7, T9-T10) and lumbar levels (T12-L1, L2-L3, L5-L6) were tested in rhesus monkeys A182(□), N75(△), and A322(○) and in baboons H40(■) and H54(●). The bar(—) indicates the maximum cyclic stress.

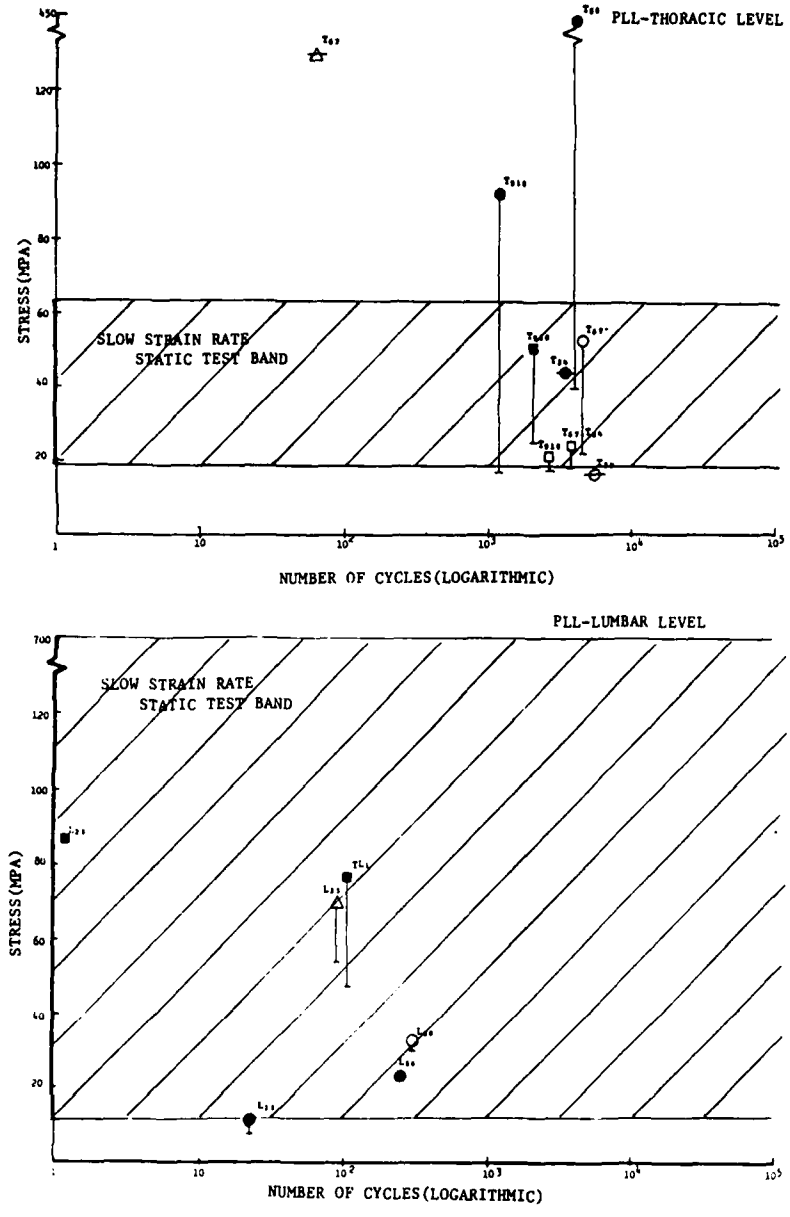

Figure 4: Failure Stress Versus Number of Cycles for Thoracic and Lumbar Posterior Longitudinal Ligaments (P.L.L.) from Three Rhesus Monkeys and Two Baboons. The P.L.L. at the thoracic levels (T3-T4, T6-T7, T9-T10) and lumbar levels (T12-L1, L2-L3, L5-L6) were tested in rhesus monkeys A182 (□), N75 (△), and A322 (○) and in baboons H40 (■) and H54 (●). The bar (—) indicates the maximum cyclic stress.

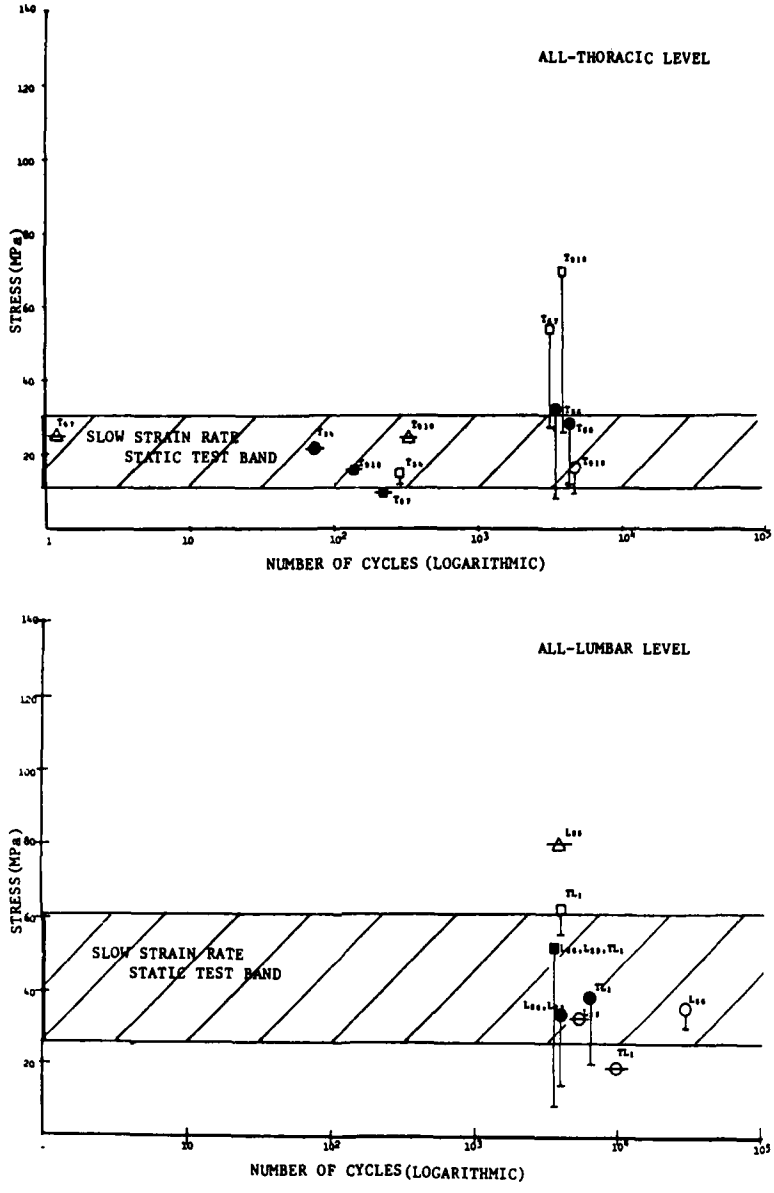

Figure 5: Failure Stress Versus Number of Cycles for Thoracic and Lumbar Anterior Longitudinal Ligaments (A.L.L.) from Three Rhesus Monkeys and Two Baboons. The A.L.L. at the thoracic levels (T3-T4, T6-T7, T9-T10) and lumbar levels (T12-L1, L2-L3, L5-L6) were tested in rhesus monkeys A182(□), N75(△), and A322(○) and in baboons H40(■) and H54(●). The bar(—) indicates the maximum cyclic stress.

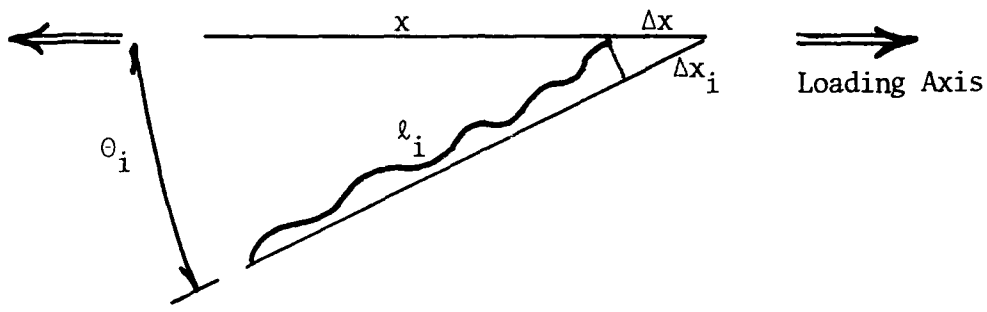

Figure 6. Collagen Fiber Geometry.

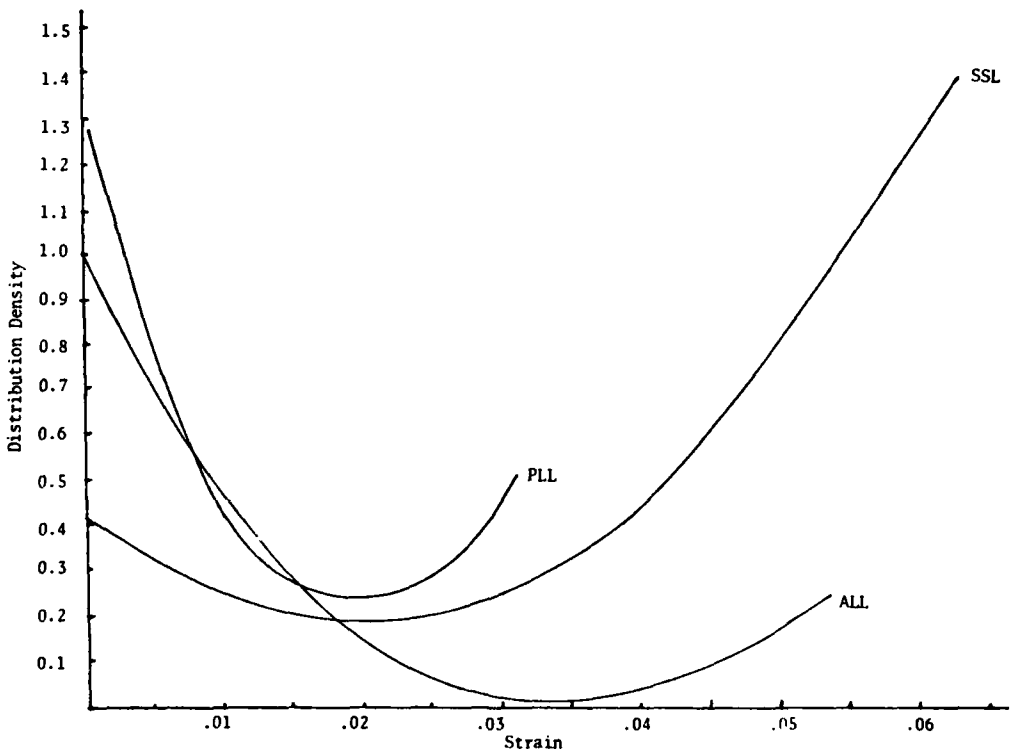

Figure 7. Distribution Functions for Spinal Ligaments.

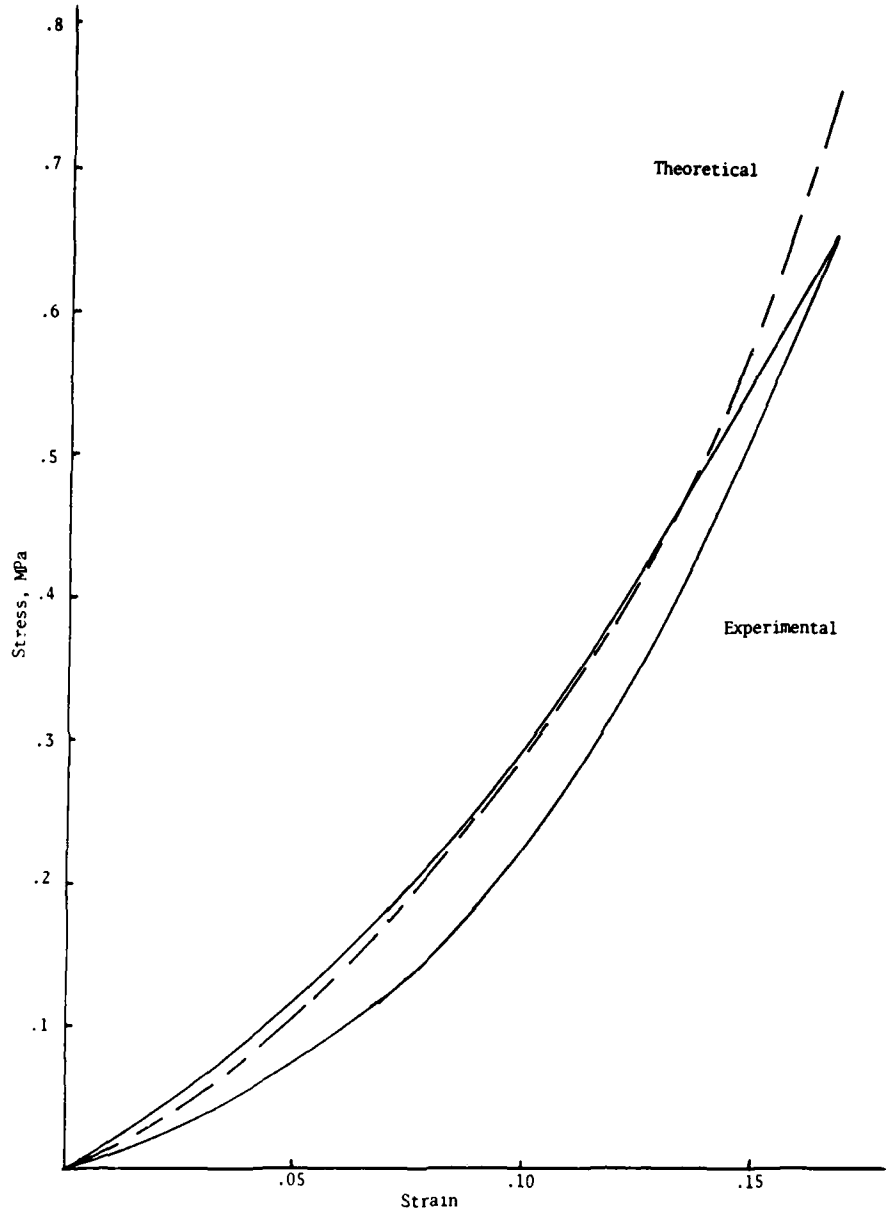

Figure 8. 100%/sec. Strain Rate Response of a Human Anterior Longitudinal Ligament (L1 - L2)

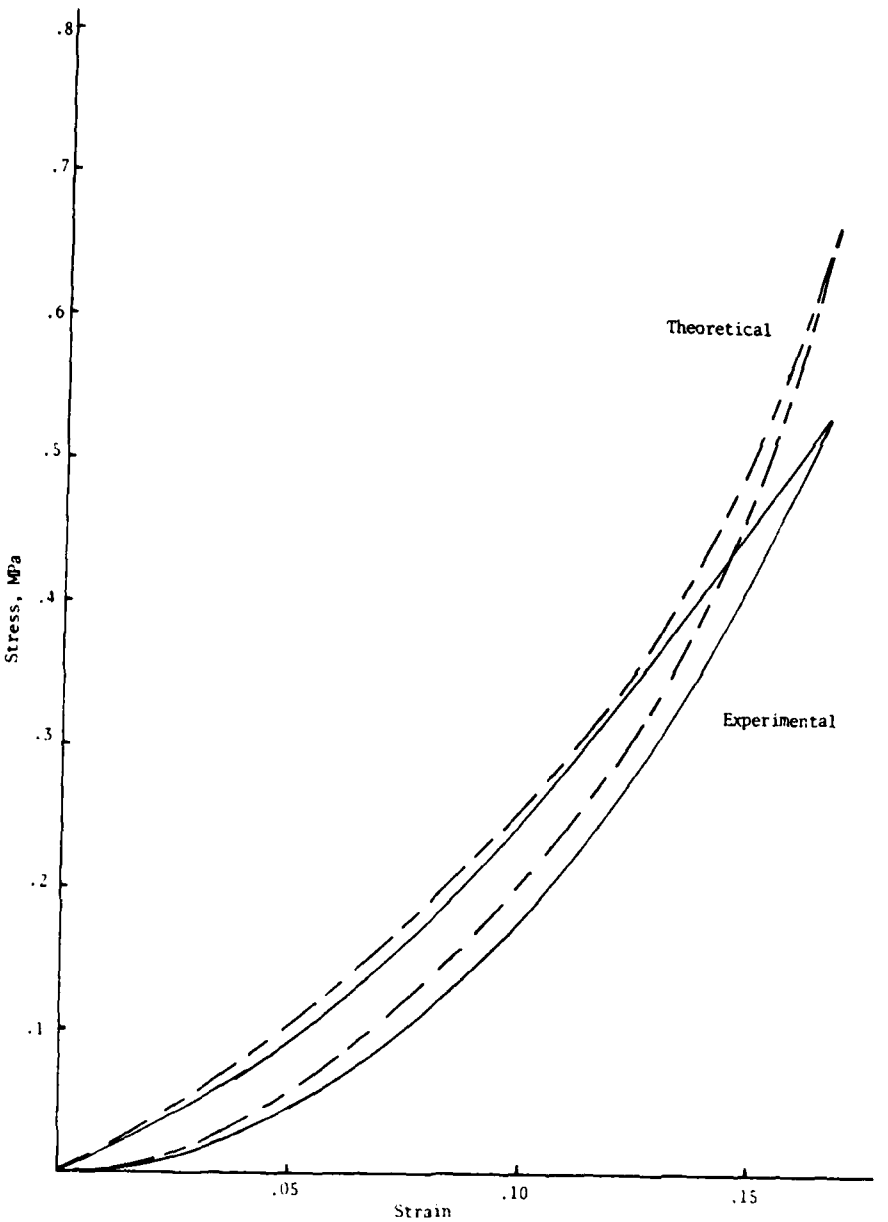

Figure 9. 1%/sec. Strain Rate Response of a Human Anterior Longitudinal Ligament (L1 - L2)

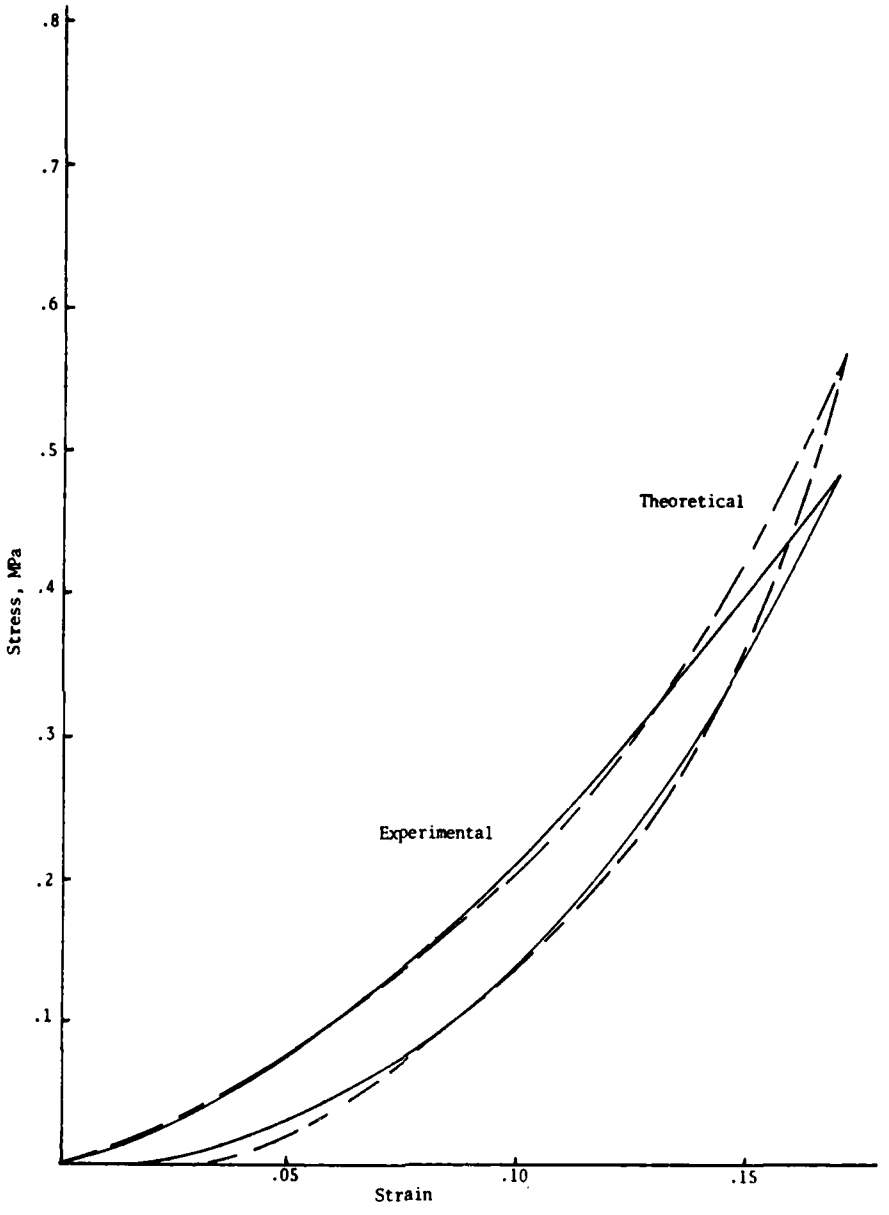

Figure 10. 0.1 %/sec. Strain Rate Response of a Human Anterior Longitudinal Ligament (L1 - L2)

Table 2. Single Extension of Spinal Ligaments from Rhesus U70.

Spinal Ligament	Failure Load (N)	Cross-Sectional Area (mm^2)	Failure Stress (MPa)	Extension at Failure (mm)
SSL				
C7/T1		0.301		
T3/T4	9.1	0.394	23.2	2.24
T6/T7	15.6	0.419	37.1	0.99
T9/T10	25.8	0.477	54.0	1.04
T12/L1	11.3	0.590	19.2	2.08
L2/L3	26.2	0.247	106.2	2.44
L5/L6	15.6	0.271	57.5	4.19
LF				
C7/T1	129.0	6.72	19.2	3.76
T3/T4	83.2	6.49	12.8	2.24
T6/T7	81.8	4.94	16.6	3.66
T9/T10	242.0	12.90	18.8	4.19
T12/L1	294.0	14.90	19.7	3.68
L2/L3	702.0	31.20	22.5	5.08
L5/L6	382.0	25.30	15.1	5.36
PLL				
C7/T1	80.1	2.41	33.3	0.76
T3/T4	71.0	1.61	44.0	1.83
T6/T7	57.2	0.90	63.4	1.12
T9/T10		1.47		
T12/L1		1.96		
L2/L3	19.6	1.62	11.5	1.14
L5/L6	101.0	1.31	77.1	1.68
ALL				
C7/T1	53.6	4.83	11.1	1.75
T3/T4	136.1	7.02	19.4	3.33
T6/T7	203.5	10.3	19.9	3.12
T9/T10	494.6	11.1	44.7	4.93
T12/L1	655.6	10.8	60.5	3.53
L2/L3	381.6	12.3	30.9	4.17
L5/L6	321.2	10.1	31.7	3.79

Table 3. Single Extension of Spinal Ligaments from Rhesus U88.

Spinal Ligament		Failure Load (N)	Cross-Sectional Area (mm^2)	Failure Stress (MPa)	Extension at Failure (mm)
SSL					
	C7/T1	32.9	0.265	124.5	6.07
	T3/T4	20.1	0.367	54.8	5.46
	T6/T7	36.5	0.710	51.4	3.81
	T9/T10	11.6	1.280	9.0	3.30
	T12/L1	16.0	1.670	9.6	5.21
	L2/L3	21.4	0.678	31.5	4.45
	L5/L6	37.5	0.678	55.3	3.61
LF					
	C7/T1*		2.64		
	T3/T4*	113.0	6.25	18.1	5.84
	T6/T7*	258.9	11.40	22.8	4.06
	T9/T10*		16.70		
	T12/L1*	489.3	20.60	23.8	3.56
	L2/L3*	658.3	41.30	15.9	4.32
	L5/L6	601.4	41.30	14.6	4.29
	*Sample was split, loads added, extensions averaged.				
PLL					
	C7/T1	43.3	0.975	44.5	1.09
	T3/T4	59.2	1.480	39.9	1.78
	T6/T7		1.460		
	T9/T10		1.540		
	T12/L1	24.9	2.110	11.8	1.65
	L2/L3	207.3	0.301	688.0	1.52
	L5/L6	114.8	0.301	380.9	2.22
ALL					
	C7/T1	90.5	5.4	16.9	1.73
	T3/T4	259.2	8.6	30.1	2.41
	T6/T7	386.1	13.3	29.0	2.79
	T9/T10	658.3	18.5	35.5	3.94
	T12/L1	581.8	22.3	26.1	4.32
	L2/L3	676.1	13.3	50.9	4.19
	L5/L6	770.4	13.3	58.0	6.60

Table 4. Cyclic Loading of Spinal Ligaments from Rhesus N75.

Spinal Ligament	Cyclic Load Range Max (N)	Cyclic Load Range Min (N)	Cross-Sectional Area (mm^2)	Cyclic Stress Range Max (MPa)	Cyclic Stress Range Min (MPa)	Failure Stress (MPa)	Number of Cycles
SSL							
T3/T4							
T6/T7			0.37				
T9/T10			0.32				
T12/L1	35.4	6.2	0.27	129.8	22.7	129.8	3
L2/L3			0.45				
L5/L6	49.4	35.0	0.52	94.4	66.9	94.4	2
LF							
T3/T4							
T6/T7			4.79				
T9/T10	92.7	46.3	7.58	12.2	6.1	12.2	7,700
T12/L1			10.40				
L2/L3			12.20				
L5/L6			13.2				
PLL							
T3/T4							
T6/T7	32.7	23.7	0.252	129.8	94.0	129.8	65
T9/T10			3.10				
T12/L1			2.34				
L2/L3	133.4	41.9	1.92	69.6	21.9		95
L5/L6			1.65				
ALL							
T3/T4							
T6/T7	208.2	158.6	8.18	25.5	19.4	25.5	3
T9/T10	281.8	248.2	11.40	24.7	21.8	24.7	343
T12/L1	423.9	302.5	11.80	35.8	25.6	35.8	3
L2/L3			5.74				
L5/L6	390.1	274.6	4.90	79.6	56.0		4,000

Table 5. Cyclic Loading of Spinal Ligaments from Rhesus A182.

Spinal Ligament	Cyclic Load Range Max (N)	Cyclic Load Range Min (N)	Cross-Sectional Area (mm^2)	Cyclic Stress Range Max (MPa)	Cyclic Stress Range Min (MPa)	Failure Stress (MPa)	Number of Cycles
SSL							
T3/T4			0.437				
T6/T7	15.3	8.7	0.559	27.3	15.5		4,771
T9/T10	12.8	3.3	0.561	22.8	5.8		9,100
T12/L1	24.1	3.0	0.561	42.9	5.4		4,400
L2/L3	15.3	2.5	0.703	21.7	3.6	22.1	120
L5/L6	14.1	2.5	0.703	20.1	3.6		29,160
LF							
T3/T4			3.8				
T6/T7			4.6				
T9/T10			11.2				
T12/L1	389.9	266.4	16.7	23.3	15.9	27.7	1,100
L2/L3	378.8	262.6	23.6	16.1	11.1		32,451
L5/L6	380.8	260.1	23.6	16.1	11.0	19.8	35,000
PLL							
T3/T4	47.8	32.9	2.0	23.6	16.2		5,700
T6/T7	43.3	28.6	2.0	21.4	12.7	53.6	4,300
T9/T10			2.8			19.6	0
T12/L1			3.3			12.8	0
L2/L3			2.2			29.8	0
L5/L6	66.5	46.3	2.2	30.4	21.1	31.0	300
ALL							
T3/T4			6.8			21.7	0
T6/T7	198.7	138.2	13.8	14.4	10.0		4,650
T9/T10	204.8	146.6	20.7	9.9	7.1	17.5	4,500
T12/L1	407.8	289.6	21.2	19.2	13.6		10,000
L2/L3	436.0	293.4	13.1	33.3	22.4		5,400
L5/L6	406.2	174.7	13.1	31.0	13.3	36.0	30,000

Table 6. Cyclic Loading of Spinal Ligaments from Rhesus A322.

Spinal Ligament	Cyclic Load Range Max (N)	Cyclic Load Range Min (N)	Cross-Sectional Area (mm^2)	Cyclic Stress Range Max (MPa)	Cyclic Stress Range Min (MPa)	Failure Stress (MPa)	Number of Cycles
SSL							
T3/T4			1.30				
T6/T7			1.86				
T9/T10	10.8	9.8	0.36	30.4	27.6	79.7	31
T12/L1	19.9	14.1	0.36	53.8	39.7	125.2	23,056
L2/L3	15.3	8.0	2.07	7.4	3.9	15.6	18
L5/L6	61.2	14.2	2.45	25.0	5.8	24.9	25
LF							
T3/T4			6.28				
T6/T7			5.99				
T9/T10			14.30				
T12/L1	236.9	183.9	14.30	16.6	12.9	20.9	14,000
L2/L3	419.0	323.8	26.80	15.7	12.1	15.7	3
L5/L6			2.46			18.2	0
PLL							
T3/T4	29.5	23.2	1.72	17.2	13.5	24.8	4,000
T6/T7	33.1	25.9	1.83	18.2	14.2	22.1	4,000
T9/T10	49.4	37.4	2.84	17.4	13.2	20.7	2,860
T12/L1			2.84			83.1	0
L2/L3			0.95			56.5	0
L5/L6	21.3	16.0	2.13	10.0	7.5	80.4	4,000
ALL							
T3/T4	138.6	106.8	10.70	12.9	10.0	13.1	300
T6/T7	220.7	172.8	8.16	27.0	21.2	53.1	3,451
T9/T10	171.7	131.0	6.55	26.2	20.0	69.4	4,000
T12/L1	364.7	280.9	6.55	55.7	42.9	62.1	4,000
L2/L3	348.7	254.2	15.50	22.5	16.4	47.5	25
L5/L6	337.4	242.2	19.60	17.2	12.4	41.0	25

Table 7. Cyclic Loading of Spinal Ligaments from Baboon H40.

Spinal Ligament	Cyclic Load Range Max (N)	Cyclic Load Range Min (N)	Cross-Sectional Area (mm^2)	Cyclic Stress Range Max (MPa)	Cyclic Stress Range Min (MPa)	Failure Stress (MPa)	Number of Cycles
SSL							
T3/T4			1.08				
T6/T7			0.71				
T9/T10			1.32				
T12/L1	206.2	144.1	1.72	119.7	83.6	119.7	214
L2/L3	287.3	211.9	2.56	112.3	82.8	112.5	50
L5/L6	191.3	136.8	3.07	62.4	44.6	62.5	3049
LF							
T3/T4	143.9	113.2	9.93	14.5	11.4	14.5	45
T6/T7			12.70				
T9/T10			9.61				
T12/L1	482.6	335.4	5.62	85.9	59.7	85.9	2
L2/L3			12.90			33.1	3
L5/L6	661.9	486.5	26.80	24.7	18.2		2010
PLL							
T3/T4			2.21				
T6/T7	114.6	90.3	4.07	28.1	22.2	28.1	1
T9/T10	106.9	76.6	4.19	25.5	18.3	51.1	2170
T12/L1	206.4	112.9	4.38	47.1	25.8	75.6	102
L2/L3			3.59			87.5	0
L5/L6			2.66			116.2	0
ALL							
T3/T4			36.60				
T6/T7	307.1	220.3	30.90	10.0	7.1	10.0	020
T9/T10	391.0	287.3	24.80	15.7	11.6	15.7	143
T12/L1	438.5	303.5	27.60	15.9	11.0	20.2	4000
L2/L3	274.0	202.1	29.20	9.2	6.9	22.1	4000
L5/L6	396.3	287.7	23.40	16.9	12.3	54.0	4005

Table 8. Cyclic Loading of Spinal Ligaments from Baboon H54.

Spinal Ligament	Cyclic Load Range Max (N)	Cyclic Load Range Min (N)	Cross-Sectional Area (mm^2)	Cyclic Stress Range Max (MPa)	Cyclic Stress Range Min (MPa)	Failure Stress (MPa)	Number of Cycles
SSL							
T3/T4			1.53				
T6/T7	70.7	52.6	1.53	46.2	34.4	46.2	1520
T9/T10	69.8	54.9	2.53	27.6	21.7	72.2	4620
T12/L1	48.5	16.3	2.37	20.5	6.9	34.8	50
L2/L3	135.9	103.8	2.36	57.6	44.0	63.9	4057
L5/L6	68.9	35.4	2.19	31.4	16.1	57.7	26
LF							
T3/T4			10.90				
T6/T7			10.10				
T9/T10			17.20				
T12/L1	301.3	229.2	25.20	12.0	9.1		3994
L2/L3			51.80				
L5/L6			72.70				
PLL							
T3/T4	66.1	48.5	1.46	45.4	33.2	49.7	3982
T6/T7	66.6	48.9	1.73	38.5	28.3		4000
T9/T10	36.3	26.1	2.22	16.4	11.8	92.4	1240
T12/L1			2.43			40.2	0
L2/L3	70.7	23.6	9.04	7.8	2.6	11.7	22
L5/L6	195.3	148.6	8.42	23.2	17.6	23.2	258
ALL							
T3/T4	206.2	159.5	9.08	22.7	17.6	22.7	75
T6/T7	201.7	159.5	17.00	11.9	9.4	28.1	3985
T9/T10	207.5	162.7	24.80	8.4	6.6	33.9	3990
T12/L1	508.3	396.8	24.60	20.6	16.1	36.9	5743
L2/L3	525.9	409.1	30.20	17.4	13.6	27.6	3985
L5/L6	529.6	414.5	36.90	14.4	11.2	34.0	3985

Table 9: Summary of Failure Stress for Single Extensions and Cyclic Loading of All Animals.

Region Ligament	Single Extension Failure Stress (MPa)	Var* (MPa)	n	Cyclic Loading Failure Stress (MPa)	Var* (MPa)	n	Combined Conditions Failure Stress (MPa)	Var* (MPa)	n
Thoracic:									
S.S.L.	50.6	36.9	7	66.0	79.7 46.2	3	55.2	32.1	10
L.F.	18.1	3.3	6	13.4	14.5	2	16.9	3.6	8
P.L.L.	45.0	11.2	5	49.2	36.3	10	47.8	29.2	15
A.L.L.	25.8	11.0	8	27.9	17.2	12	27.1	14.8	20
Lumbar:									
S.S.L.	46.6	34.9	6	71.9	43.0	12	63.5	41.2	18
L.F.	18.6	4.0	6	31.6	24.7	7	25.6	18.9	13
P.L.L.**	[233.9]	[293.6]	5	54.0	34.0	12	[106.9]	[172.9]	17
A.L.L.	43.0	15.2	6	37.9	12.8	11	39.7	13.4	17

*Variability (See text).

**Brackets indicate questionable stress values based on small and difficult to delineate ligament areas.

Table 10: Cyclic Extension at Failure.

Region Ligament	Single Extension Failure Extensn (mm)	Var* (mm)	n	Cyclic Loading Failure Extensn (mm)	Var* (mm)	n	Combined Conditions Failure Extensn (mm)	Var* (mm)	n
Thoracic:									
S.S.L.	3.27	2.01	7	2.43	3.28 1.81	3	3.02	1.73	10
L.F.	3.96	1.16	6	3.26		1	3.86	1.09	7
P.L.L.	1.32	0.47	5	1.34	0.80	9	1.33	0.68	14
A.L.L.	3.00	1.09	8	2.50	0.62	7	2.76	0.91	15
Lumbar:									
S.S.L.	3.66	1.21	6	3.14	1.62	7	3.38	1.41	13
L.F.	3.88	1.69	6	4.88	1.88	5	4.34	1.77	11
P.L.L.	1.64	0.39	5	2.00	1.16	10	1.88	0.97	15
A.L.L.	3.77	2.02	6	2.94	1.34	9	3.27	1.63	15

*Variability (See text)

Table 11: Exponential Fit of Cyclic Creep Extensions

Ligament	Level	Animal No.	Species	Cyclic max (MPa)	SHORT TERM cycles fit	SHORT TERM B1	SHORT TERM B2	SHORT TERM B2/B1	LONG TERM total cycles	LONG TERM B1	LONG TERM B2	LONG TERM B2/B1
SSL	T5/T6	H54	B	46.2	12	.015	.018	1.20	1520	.025	.028	1.12
SSL	T9/T10	A182	R	22.8	30	.064	.066	1.03	9100	.022	.026	1.18
		A322	R	30.4	31	.133	.137	1.03	31			
		H54	B	27.6	31	.063	.067	1.06	4612	.029	.032	1.10
SSL	T12/L1	A182	R	42.9	30	.037	.059	1.59	4400			
		A322	R	53.8	22	.024	.029	1.21	23,056			
		H40	B	119.7	30	.274	.347	1.27	214			
		H54	B	20.5	25	.023	.029	1.26	50			
SSL	L2/L3	A322	R	7.4	18	.032	.037	1.16	18			
		H40	B	112.3	14	.033	.052	1.58	50			
		H54	B	57.6	24	.071	.075	1.06	4057	.024	.026	1.08
SSL	L5/L6	A182	R	20.1	30	.015	.025	1.67	29,160	.047	.049	1.04
		A322	R	25.0	19	.127	.163	1.28	25			
		H40	B	62.4	21	.034	.049	1.44	3049	.068	.076	1.12
		H54	B	31.4	26	.084	.094	1.12	26			
LF	T12/L1	A182	R	23.3	30	.033	.040	1.21	1100	.056	.055	0.98
		H54	B	12.0	26	.004	.014	3.50	3994	.004	.015	3.75
LF	L2/L3	A182	R	16.1	30	.018	.018	1.00	32,451	.040	.041	1.03
LF	L5/L6	A182	R	16.1	30	.011	.011	1.00	35,000	.019	.020	1.05
		H40	B	24.7	30	.021	.029	1.38	2010	.066	.073	1.11

(continued)

Ligament	Level	Animal No.	Species	Cyclic max (MPa)	SHORT TERM cycles fit	SHORT TERM B1	SHORT TERM B2	SHORT TERM B2/B1	LONG TERM total cycles	LONG TERM B1	LONG TERM B2	LONG TERM B2/B1
PLL	T3/T4	A322	R	17.2	31	.042	.039	0.93	4000	.057	.064	1.12
		H54	B	45.4	31	.129	.144	1.12	3982	.189	.228	1.21
PLL	T6/T7	A182	R	21.4	28	.023	.030	1.30	4300	.049	.054	1.10
		A322	R	18.2	31	.090	.082	0.91	4000	.179	.204	1.14
PLL	T9/T10	A322	R	17.4	30	.061	.067	1.10	2860	.217	.225	1.04
		H40	B	25.5	31	.072	.101	1.40	2170			
PLL	T12/L1	H40	B	47.1	30	.073	.087	1.19	102			
PLL	L2/L3	N75	R	69.6	14	.055	.061	1.11	95			
		H54	B	7.8	23	.053	.063	1.19	22			
PLL	L5/L6	A182	R	30.4	30	.043	.058	1.35	300			
		A322	R	10.0	30	.042	.045	1.07	4000	.085	.094	1.11
		H54	B	23.2	31	.030	.034	1.13	258	.029	.024	0.83

(continued)

Ligament	Level	Animal No.	Species	Cyclic max (MPa)	SHORT TERM cycles fit	SHORT TERM B1	SHORT TERM B2	SHORT TERM B2/B1	LONG TERM total cycles	LONG TERM B1	LONG TERM B2	LONG TERM B2/B1
ALL	T3/T4	A322	R	12.9	31	.093	.104	1.12	300			
		H54	B	22.7	15	.117	.118	1.01	75			
ALL	T6/T7	A182	R	14.4	30	.054	.061	1.13	4650	.072	.082	1.14
		A322	R	27.0	31	.121	.125	1.03	3451	.135	.150	1.11
		H40	B	10.0	26	.076	.084	1.11	220	.075	.077	1.03
ALL	T5/T6	H54	B	11.9	31	.078	.088	1.13	3985	.092	.105	1.14
ALL	T9/T10	N75	R	24.7	31	.069	.068	0.99	343			
		A182	R	10.0	30	.068	.081	1.19	4500	.101	.123	1.22
		A322	R	26.2	31	.068	.078	1.15	4000	.098	.113	1.16
		H40	B	15.7	31	.090	.095	1.06	143			
		H54	B	8.4	31	.062	.073	1.18	3990	.119	.128	1.08
ALL	T12/L1	A182	R	19.2	30	.084	.094	1.12	10,000	.083	.084	1.01
		A322	R	55.7	18	.074	.079	1.07	4000	.037	.038	1.03
		H40	B	15.9	31	.051	.057	1.12	4000	.045	.050	1.11
		H54	B	20.6	31	.089	.091	1.02	5743	.068	.074	1.09
ALL	L2/L3	A182	R	33.3	30	.057	.070	1.23	5400	.083	.097	1.17
		A322	R		25	.081	.082	1.01	25			
		H40	B	9.2	31	.069	.072	1.04	4000	.072	.080	1.11
		H54	B	17.4	31	.066	.069	1.04	3985	.070	.075	1.07
ALL	L5/L6	A182	R	31.0	33	.052	.059	1.13	30,000			
		A322	R		25	.072	.076	1.05	25			
		H40	B	16.9	30	.064	.070	1.09	4005	.054	.058	1.07
		H54	B	14.4	31	.050	.054	1.08	3985	.074	.079	1.07

REFERENCES

1. Haut, R. C. and R. W. Little, "A Constitutive Equation for Collagen Fibers," J. Biomech., 5:423-430, 1972.

2. Woo, S. L-Y., M. A. Gomez and W. H. Akeson, "The Time and History-Dependent Viscoelastic Properties of the Canine Medial Collateral Ligament," J. Biomech. Eng., 103:293-298, 1981.

3. Fung, Y. C. B., "On the Mechanical Behavior of Elastic Animal Tissue," Trans. Soc. Rheol., 13:83-102, 1967.

4. Lanir, Y., "A Microstructure Model for the Rheology of Mammalian Tendon," J. Biomech. Eng., 102:332-339, 1980.

5. Cohen, R. E., C. J. Hooley and N. G. McCrum, "Viscoelastic Creep of Collagenous Tissue," J. Biomech., 9:175-184, 1976.

6. Pinto, J. G. and Y. C. Fung, "Mechanical Properties of the Heart Muscle in the Passive State," J. Biomech., 6(6):597-616, 1973.

7. Twomey, L., and J. Taylor, "Flexion Creep Deformation and Hysteresis in the Lumbar Vertebral Column," Spine 7(2):116-122, 1982.

8. Little, R. W., R. P. Hubbard, D. L. Hyler, and A. R. Slonim, "Mechanical Properties of Spinal Ligaments for Rhesus Monkey, Baboon, and Chimpanzee," AFAMRL-TR-81-40, Air Force Aerospace Medical Research Laboratory, Wright-Patterson AFB, Ohio, 1981.

9. Noyes, F. R., "Functional Properties of Knee Ligaments and Alterations Induced by Immobilization," AMRL-TR-76-27, Aerospace Medical Research Laboratory, Wright-Patterson AFB, Ohio, 1976.

☆U.S. GOVERNMENT PRINTING OFFICE: 1983—659-005/2033